Spontaneous Vesicle Formation of Mixtures of Double-Chain Cationic Surfactants with a Different Counterion

Makoto Aratono,*,† Azusa Mori,† Ikuyo Koga,† Makiko Shigehisa,† Nami Onimaru,† Koji Tsuchiya,‡ Takanori Takiue,† and Hiroki Matsubara†

Department of Chemistry, Faculty of Sciences, Kyushu University, Fukuoka 812-8581, Japan and Department of Pure and Applied Chemistry, Faculty of Science and Technology, Tokyo University of Science, Chiba 278-8510, Japan

Received: April 22, 2008; Revised Manuscript Received: June 3, 2008

Aggregate formation of a didodecyldimethylammonium bromide (DDAB) and didodecyldimethylammonium chloride (DDAC) mixture in aqueous solution was investigated. The concentration vs composition diagram of aggregate formation was constructed by analyzing the surface tension, turbidity, and electrical conductivity data. The cryogenic transmission electron microscopy was applied to several representative points in the diagram and provided information of the morphology of aggregates. The sequence of monomer (m) − m + small aggregate (A) − m + A + vesicle (V) − m + V was concluded with increasing total concentration of surfactants at all mixing ratios. The compositions of counterions in A and V were estimated on the basis of thermodynamic consideration and examined from the viewpoint of asymmetry of constituents and uneven distribution between outer and inner monolayers of a vesicle bilayer. Vesicle surfaces were suggested to abound in chloride ions compared to bulk solution, which is opposite to spherical micelle surfaces.

Introduction

Spontaneous vesicle formation of a synthetic surfactant[1–5] has been an important issues of surfactant sciences since Talmon et al. found that of dialkyldimethylammonium hydroxide at higher pH.[6] Israleachivilli suggested that forming a closed bilayer with a finite surfactant molecules from an open planer bilayer with infinite ones is not only energetically but also entropically favorable because water-edge contact of the latter is reduced and one planner bilayer can produce many vesicle particles.[7] Considering a vesicle particle has two monolayers with an opposite sign of curvature, however, it is evident that the bending energy of such monolayers has a certain contribution to the free energy of vesicle formation.[8,9] A detailed molecular theory of the bending properties of one component charged surfactant has been developed recently with respect to equilibrated (thermodynamically opened) monolayers and vesicles of finite thickness; it was demonstrated that the bending properties are dependent strongly on the flexibility of the surfactant hydrophobic tail, and the spontaneous curvature is reduced when it is flexible.[10]

In binary surfactant mixtures, spontaneous vesicle formation is expected to take place more easily than in single surfactant systems because an uneven distribution of different surfactants is possible between two monolayers having an opposite sign of curvature. Typical combinations experimentally investigated are double-long-chain salts ($R_1^+R_2^-$),[11] cationic and anionic surfactants mixtures ($R_1^+X^- + M^+R_2^-$),[12–21] single-chain and double-chain surfactant mixtures ($R^+X^- + (R_1R_2)^+Y^-$),[14,22,23] binary double-chain surfactant mixtures ($(R_1R_1)^+X^- + (R_2R_2)^+X^-$),[24] and so on. In the first and second cases, the respective single surfactants do not form vesicles solely but their mixtures do. In the third case, the surfactant R^+X^- that does not form vesicles by itself enhances more the vesicle formation of $(R_1R_2)^+Y^-$. In the fourth case, both of them form vesicles but the composition of the vesicle bilayer is significantly changed by the other. From a theoretical viewpoint, Safran et al. investigated the effect of surfactant mixing on the bending properties of mono- and bilayers and demonstrated the relationship between the effective bilayer bending constant and bending rigidity due to different compositions in outer and inner monolayers.[25,26] Furthermore, Bergström extended his theory on one-component vesicle formation to different kinds of binary mixtures and demonstrated thoroughly that effective bilayer bending constants are considerably reduced for thermodynamically open vesicles, and as a consequence, the compositions in outer and inner monolayers are different from each other for minimizing the free energy in each monolayer.[27–29]

Spontaneous vesicle formation of a dodecyltrimethylammonium bromide (DTAB) and didodecyldimethylammonium bromide (DDAB) mixture of the type of $R^+X^- + (R_1R_2)^+X^-$ was reported in our previous paper.[23] The concentration vs composition diagram of aggregate formation was constructed using and analyzing the data on surface tension, turbidity, and electrical conductivity. It was shown clearly that addition of DTAB to DDAB solution lowered considerably the DDAB concentration of the vesicle formation and more surprisingly was that vesicle formation takes place directly from monomer solution in the DTAB-rich region. The uneven distribution of R^+ and $(R_1R_2)^+$ is unambiguously responsible for it. Similarly, it was demonstrated in the mixture of type of $R^+X^- + (R_1R_2)^+Y^-$, where the counterion is different from each other, that addition of dodecyltrimethylammonium chloride (DTAC) to DDAB solution lowered considerably the DDAB concentration of the vesicle formation, but the magnitude of lowering was smaller than that of the DTAB−DDAB system.[30]

It should be noted here that an uneven distribution of not only surfactant ions but also counterions is possible for the

* To whom correspondence should be addressed. Phone/fax: +81 92 642 2577. E-mail: aratono@chem.kyushu-univ.jp.
† Kyushu University.
‡ Tokyo University of Science.

10.1021/jp803484b CCC: $40.75
Published on Web 09/05/2008

DTAC−DDAB mixture. Therefore, it is not clear which is more influential on vesicle formation; both of them synergetically may enhance vesicle formation, or one of them is principally important and another is subsidiary. Although ideal mixing of counterions has been suggested in micelle formation of the DTAB and DTAC mixture,[31,32] there is only one monolayer having positive curvature corresponding to an outer monolayer of vesicles, and therefore, it is an open question whether these counterions are mixed ideally even in vesicles. In order to shed light on these unsolved problems, we investigated the vesicle formation of the DDAB−DDAC system using a basically similar experimental strategy and some thermodynamic equations that were newly developed to estimate monomer and vesicle compositions.

Experimental Section

Materials. DDAB was purchased from ACROS Organics (USA) and purified by recrystallizing it from ethyl acetate. The elemental analysis of the final product was found as C, 67.35 (calcd 67.50); H, 12.12 (calcd 12.20); N, 2.96 (calcd 3.03).

DDAC was synthesized by refluxing the reactant mixture of dodecyldimethylamine and chlorododecane[33] in ethanol for 380 h. The reactants (Tokyo Kasei Kogyo Co., Ltd. (Japan)) were distilled around 538.15 K at 2.1 mmHg and 396.15 K at 4.4 mmHg, and their purities were confirmed to be more than 99.5% by gas−liquid chromatography (column, Unisol-400). The product was carefully recrystallized six times from the diethyl ether/ethyl acetate (7/3 volume ratio) mixture and then freeze dried after washing DDAC powders twice with hexane. No endothermic peak was observed around the melting points of the reactants (dodecyldimethylamine, 253.15 K; chlorododecane, 263.85 K) on the DSC curve. The elemental analysis was found as C, 74.09; H, 13.40; N, 3.38, which was coincident with the calculated values of $9C_{26}H_{56}ClN\cdot H_2O$ (calcd C, 74.32; H, 13.49; N, 3.33) compared to $C_{26}H_{56}ClN$ (calcd C, 74.67; H, 13.50; N, 3.35). The moisture measured by the Karl Fischer method was 4563 ppm and in accord with 4796 ppm of $9C_{26}H_{56}ClN\cdot H_2O$.

Sample solutions were prepared by diluting a stock solution at the given total molality of surfactant $\hat{m}$ and the composition of DDAC $\hat{X}_2$ defined by

$$\hat{m} = m_D + m_{Br} + m_{Cl} = 2m_1 + 2m_2 \quad (1)$$

and

$$\hat{X}_2 = 2m_2/\hat{m} \quad (2)$$

where m_D, m_{Br}, and m_{Cl} are the molalities of didodecyldimethyl ammonium, bromide, and chloride ions and $m_1$and m_2 are those of DDAB and DDAC, respectively. Required amounts of DDAB and DDAC dried under vacuum at 338 K were weighted, dissolved in water, and left at least for 6 h in the air-conditioned room around 298 K to make the aqueous solution homogeneous. Sonication was not applied to avoid forming vesicles in a nonequilibrium situation. The sample solution prepared was permitted to stand for several hours to several days until the surface tension, electrical conductivity, and turbidity measurements provided constants values within the experimental errors.

Water employed in this study was distilled 3 times; water passed through an ion-exchange filter was simply distilled and then done under the presence of small amounts of potassium permanganate and sodium hydroxide in the second and third steps.

Surface Tension. The surface tension γ of the aqueous solution was measured as a function of $\hat{m}$ and $\hat{X}_2$ at 298.15 K under atmospheric pressure using the drop volume method and drop shape analysis of a pendant drop. The reproducibility of the surface tension at lower concentrations was not good enough for our purposes, and thus, only the results at higher concentrations, where the γ values from the two methods almost coincide with each other, will be demonstrated and employed in this paper.

Turbidity. Turbidity τ was measured by the turbidimeter (HACH 2100P, its light source was the tungsten filament lamp) on the basis of the ratio nephelometric method and defined by

$$\tau = I_{90}/(d_1 I_t + d_2 I_{90}) \quad (3)$$

where I_t and I_{90} are the detector currents of the transmitted light and scattered one at 90° and d_1 and d_2 are the calibration coefficients, respectively. Sample solutions for turbidity measurements were left in the air-conditioned room around 298 K at least 2 days to have a constant τ value. The experimental error was ±1% of the τ value or 0.01 nephelometric turbidity unit (NTU), where the τ value of Formazin standard solution is 4000 NTU.[34] When a sample solution is isotropic and dilute, τ is given by

$$\tau = (128\pi^5 a^6 N_V/3\lambda^4)(n^2-1)^2/(n^2+2)^2 \quad (4)$$

where λ, a, N_V, and n are the wavelength of unpolarized incident light, particle radius, number of particles per unit volume, and refractive index of particles relative to that of the surrounding medium.[35]

Conductivity. Conductivity κ measurement was performed by the conductmeter CM-60G (TOA-DKK Ltd.), and the experimental error of κ was ±0.5% of the full scale. A suitable amount of the higher concentration solution was successively injected into the lower one, and the κ value was measured twice every 10 min for each concentration.

Cryogenic Transmission Electron Micrography (Cryo-TEM). Cryogenic electron transmission microscopy (cyro-TEM) was performed at the Tokyo University of Science by means of H-7650 TEM (Hitachi High-Technologies Co., Ltd.) equipped with the cryotransfer attachment CT-3500 (Oxford Instruments) using low-dose conditions below 103 K. A small amount of sample solution was dropped on a hydrophilic microgrid, and after soaking up excess liquid by a filter paper, it was plunged very quickly into liquid ethane with EM-CPC (LEICA Ltd.).

Results

Surface Tension. The surface tension of the mixtures is plotted against $\hat{m}$ in a logarithmic scale at given $\hat{X}_2$ values in Figure 1. All the curves have a break point, which is referred to as point II hereafter, and γ becomes almost constant at concentrations above II. Judging from that the $\hat{m}$ value of II of the DDAB system was almost equal to the onset of vesicle formation (m_A^{A+V} in our previous paper)[23] and the solutions were colorless and transparent below II but bluish above II at all $\hat{X}_2$, it is reasonably assigned that vesicle particles starts to form at around II in the aqueous solutions being composed of small aggregates and monomers. Let us designate the total molality at II by $\hat{m}^{II}$. The $\hat{m}^{II}$ values are summarized in Table 1.

Turbidity. The turbidity τ is plotted against $\hat{m}$ at given compositions in Figure 2. It is almost zero in the lower concentrations and starts to increase at a certain $\hat{m}$ with increasing concentration. Looking closely at these curves and also at the $\Delta\tau/\Delta\hat{m}$ vs $\hat{m}$ curves, two characteristic concentrations $\hat{m}^{II}$ and $\hat{m}^{III}$ are specified at II and III as illustrated for $\hat{X}_2 = 0.4$ in Figure 3. The $\Delta\tau/\Delta\,\hat{m}$ value is zero at concentrations below a break point II, increases with $\hat{m}$ between II and III, and then

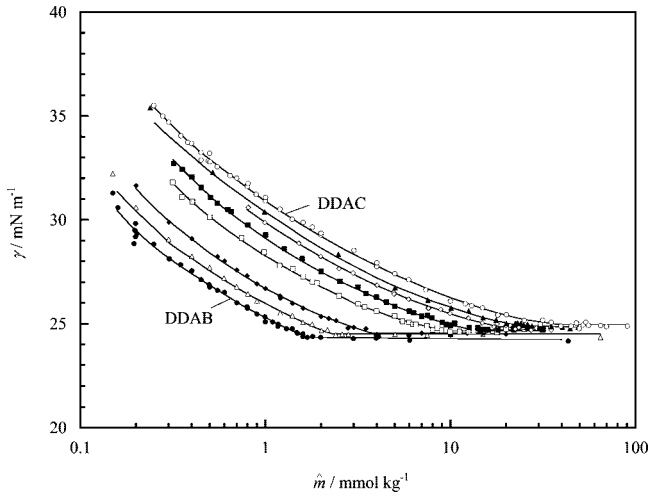

Figure 1. Surface tension vs molality curves at constant compositions: $\hat{X}_2$ = (●) 0 (DDAB), (Δ) 0.2, (♦) 0.4, (□) 0.7, (■) 0.8, (◇) 0.9, (▲) 0.95, (○) 1 (DDAC).

TABLE 1: Concentration (mmol kg^{-1}) vs Composition Values from Different Techniques

		$\hat{X}_2$							
		0.00	0.20	0.40	0.70	0.80	0.90	0.95	1.00
$\hat{m}^{III}$	τ		13.40	12.73	17.36	21.40	26.50	32.40	56.10
	κ	11.54	12.34	12.85	18.50	21.53	27.42	31.03	
	ave	11.54	12.87	12.79	17.93	21.47	26.96	31.72	56.10
	γ	1.68	2.34	3.76	9.33	12.88	17.78	23.99	42.17
$\hat{m}^{II}$	τ	1.62	2.40	3.49	8.51	12.59	18.10	22.70	46.52
	μ	1.63	2.30	3.29	9.52	14.37	16.77	22.79	
	ave	1.65	2.35	3.51	9.12	13.28	17.55	23.16	44.35
$\hat{m}^{I}$	κ	0.17	0.17	0.16	0.19	0.18	0.18	0.18	0.24

becomes almost constant above III. Since τ values are 0.5 NTU at most for normal micelle solutions, the increase in τ suggests formation of large aggregates in the solutions. The concentrations at II are almost coincident with those determined by the surface tension curves as summarized in Table 1. Although it is not evident only from the γ, τ, and $\Delta\tau/\Delta\hat{m}$ curves what kind of change happens in the solution state, the most probable one is that small aggregates and monomers grow up into vesicles between II and III and all the small aggregates are consumed for this growing up process during the increase in $\hat{m}$ from $\hat{m}^{II}$ to $\hat{m}^{III}$. The concentrations $\hat{m}^{III}$ (m^{V}_{A+V} in our previous paper[1]) are summarized in Table 1.

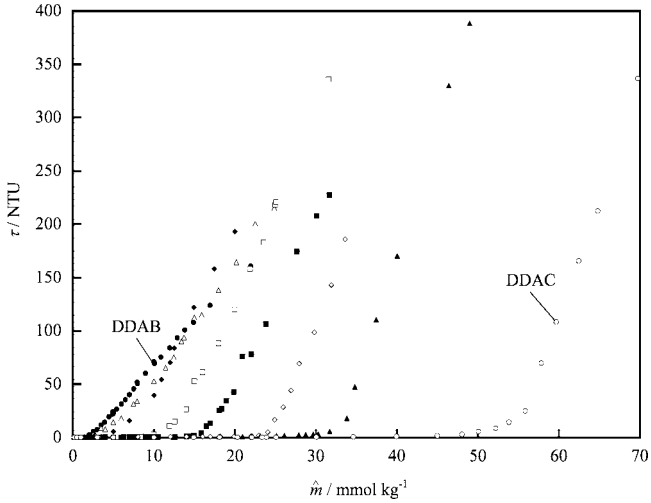

Figure 2. Turbidity vs total molality curves at constant compositions. Symbols are given in Figure 1.

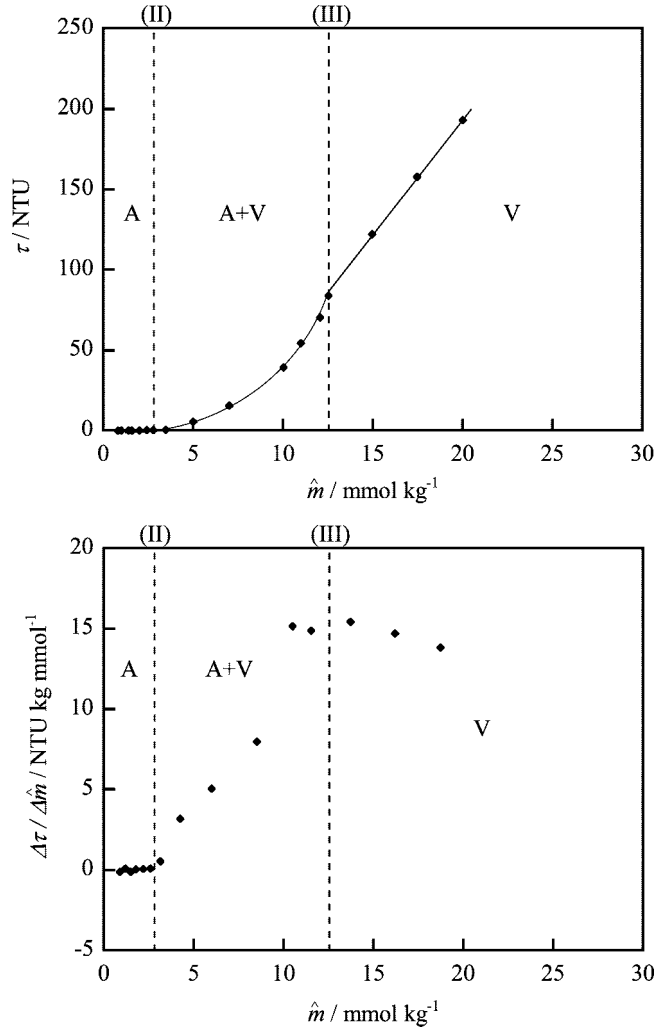

Figure 3. Turbidity (top) and differential turbidity (bottom) vs molality curves at $\hat{X}_2 = 0.4$: (A) small aggregates, (A + V) existence of small aggregates and vesicles, (V) vesicles.

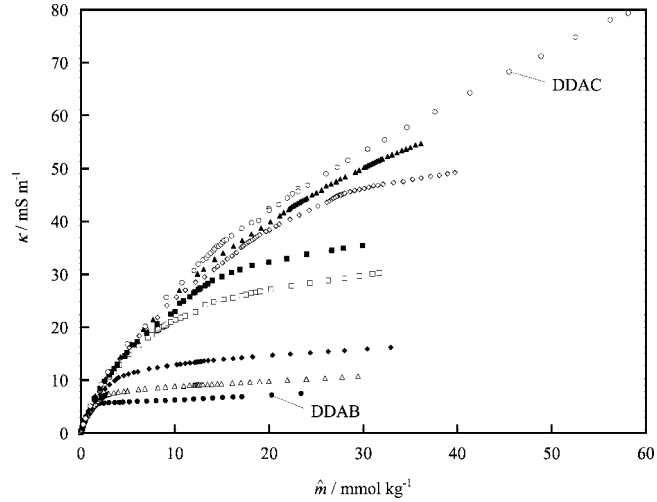

Figure 4. Specific conductivity vs molality curves at constant compositions. Symbols are given in Figure 1.

Electric Conductivity. The electrical conductivity κ vs $\hat{m}$ curves at given compositions are shown in Figure 4. The κ values of the respective pure surfactants at higher concentration regions are much different due to the difference of the

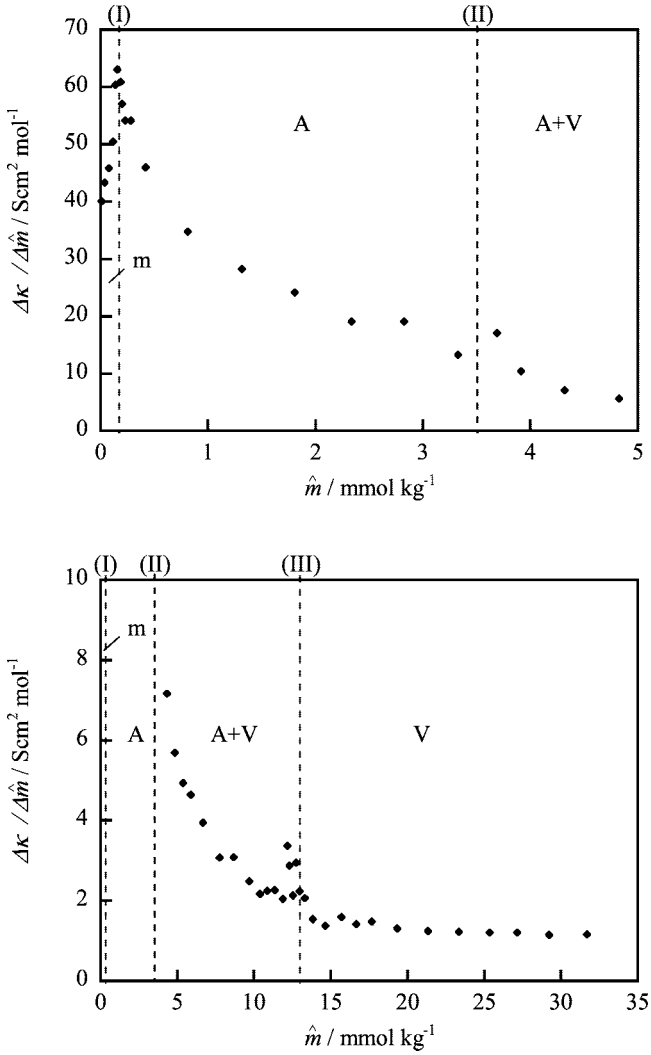

Figure 5. Differential conductivity vs molality curves at $\hat{X}_2 = 0.4$: (top) plots at lower concentrations, (bottom) plots at higher concentrations.

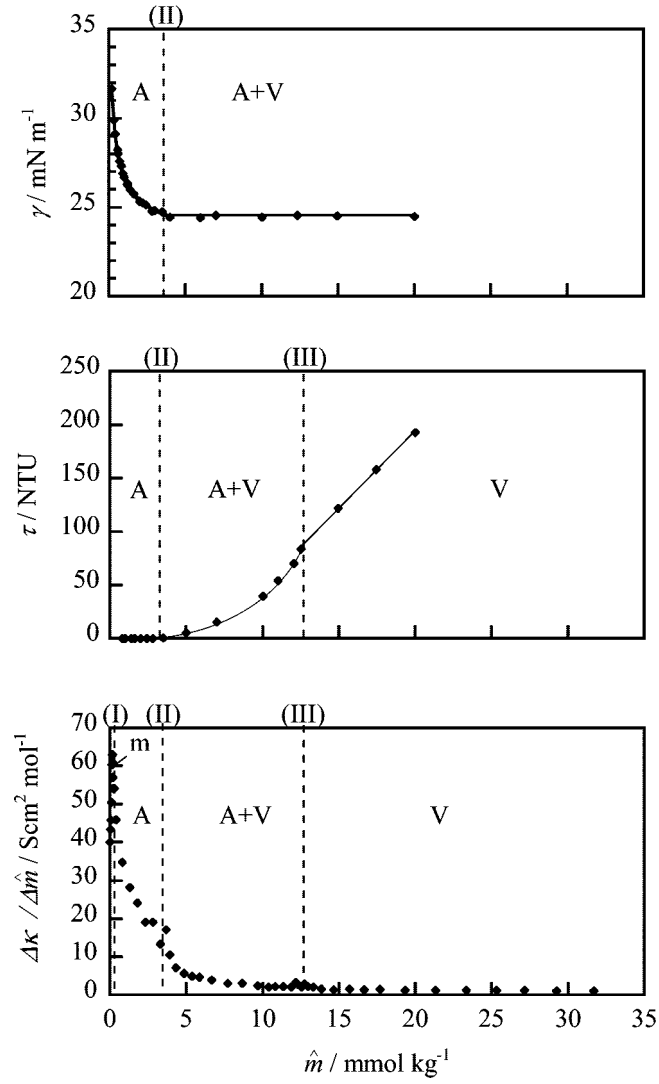

Figure 6. Correlation among surface tension (top), turbidity (middle), and differential conductivity (bottom) vs molality curves at $\hat{X}_2 = 0.4$.

concentrations of aggregate formation (that is, monomer concentrations) and the degree of counterion binding.[36] The κ values of mixtures change regularly with $\hat{X}_2$. The differential conductivity $\Delta\kappa/\Delta\hat{m}$ vs $\hat{m}$ curves are more advantageous than the conductivity curves themselves in order to specify the concentrations at which a transition in the solution state takes place; a sharp maximum at I, a sharp inflection point after the maximum at II, and a boundary between the decrease and constancy in $\Delta\kappa/\Delta\hat{m}$ at III, respectively, correspond to formation of small aggregate, the onset of vesicle formation, and the end point of the existence of small aggregates.[23] The representative $\Delta\kappa/\Delta\hat{m}$ is demonstrated at $\hat{X}_2 = 0.4$ in Figure 5. The concentrations thus determined are summarized in Table 1.

Concentration vs Composition Diagrams. Figure 6 illustrates the correspondence of the changes in γ, τ, and $\Delta\kappa/\Delta\hat{m}$ at $\hat{X}_2 = 0.4$ at the transition points. The characteristic features are similar also at other compositions. Examining the concentrations specified here comprehensively in reference to our previous study,[23] the points I, II, and III were determined to be the onset of small aggregate formation, the onset of the vesicle formation, and the end of existence of small aggregates, respectively. The concentrations at these points are designated as $\hat{m}^{\mathrm{I}}$, $\hat{m}^{\mathrm{II}}$, and $\hat{m}^{\mathrm{III}}$ ($m_{\mathrm{m}}^{\mathrm{A}}$, $m_{\mathrm{A}}^{\mathrm{A+V}}$, and $m_{\mathrm{A+V}}^{\mathrm{V}}$ in our previous paper). These values are summarized in Table 1. We note that the values estimated from the different methods coincide with each other. The average values are plotted against $\hat{X}_2$ in Figure 7.

It is realized at all compositions from the pure DDAB to the pure DDAC that the solution state is changed from the monomer solution (m) to the small aggregate + monomer solution (A) at $\hat{m}^{\mathrm{I}}$, from A to the small aggregate + vesicle + monomer solution (A + V) at $\hat{m}^{\mathrm{II}}$, and then from A +V to the vesicle + monomer solution (V) at $\hat{m}^{\mathrm{III}}$ with increasing total concentration of surfactants $\hat{m}$.

CryoTEM Observations. The existence of vesicles was confirmed by CryoTEM observations at several representative points as displayed in Figure 8. In the image at $\hat{X}_2 \approx 0.4$ and $\hat{m} \approx 6$ mmol kg^{-1} ($P_{0.4}^{6}$) it is seen that although there are many small vesicles, size is widely spread from small (~10 nm in diameter) to very large (~several hundreds of nanometers) ones and there exist vesicles in which a smaller vesicle is included. In $P_{0.4}^{59}$ the size becomes large as a whole, its distribution becomes rather narrow, and almost all vesicle particles contain smaller vesicle(s). $P_{0.8}^{59}$ shows a pattern like a fingerprint, and vesicles seem to be densely packed. The image in P_{1}^{59} shows the existence of large vesicles rather loosely packed, which is totally different from that of $P_{0.8}^{59}$.

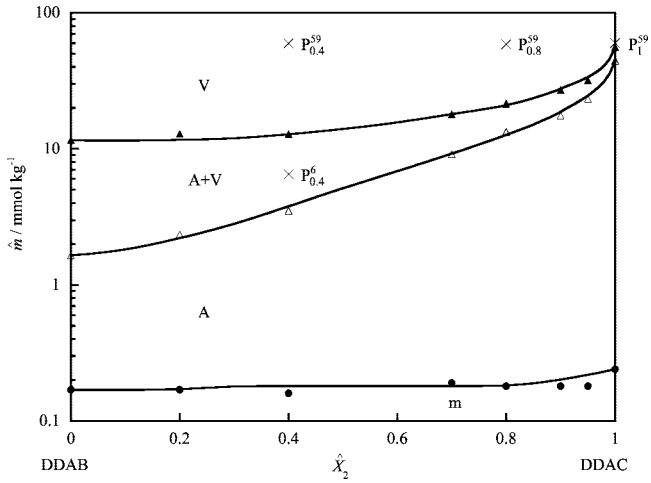

Figure 7. Concentration vs composition diagrams of aggregate formation: (●) $\hat{m}^{I}$, (Δ) $\hat{m}^{II}$, (▲) $\hat{m}^{III}$; (m) monomers, (A) small aggregates, (A + V) existence of small aggregates and vesicles, (V) vesicles. $P^{\hat{m}}_{\hat{X}}$s show the points of which CryoTEM images are displayed in Figure 7.

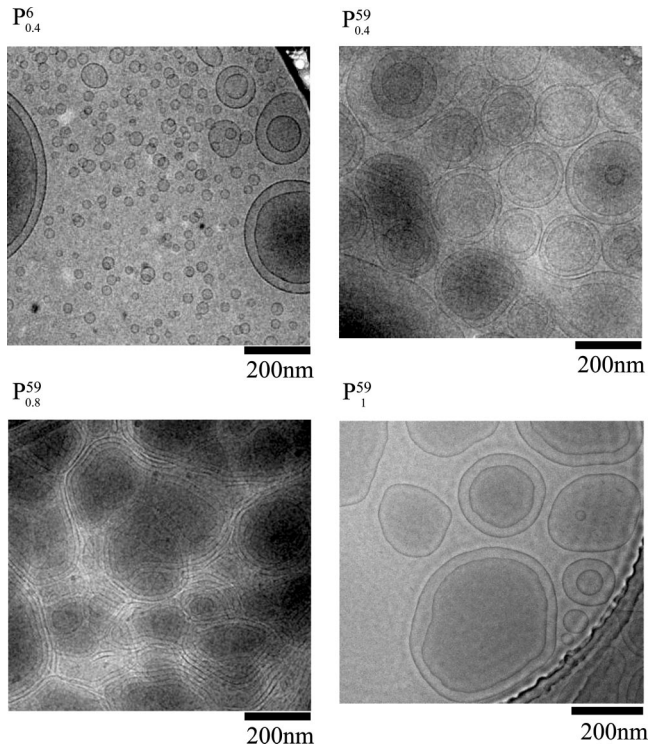

Figure 8. CryoTEM images at the representative points in the concentration vs compostion diagrams of aggregate formation.

Discussion

Small Aggregates Formation of the DDAB−DDAC System. Although the existence of small aggregates is not self-evident from the surface tension curves shown in Figure 1, the downwardly convex shape of the γ vs log $\hat{m}$ curves in Figure 1 is probably indicative of the existence of small aggregates because γ of a monomer solution is decreased almost linearly or upward convexly with increasing log $\hat{m}$, and on the other hand, γ of a micelle (large aggregates) solution is almost constant above the critical micelle concentration. On the basis of the thermodynamic consideration on adsorption from small aggregate solutions,[37] the average aggregation number was estimated by applying

$$\bar{N} = (\partial\gamma/\partial\log\hat{m})_{\hat{m}<\hat{m}^{I}}/(\partial\gamma/\partial\log\hat{m})_{\hat{m}>\hat{m}^{I}} \quad (5)$$

to the surface tension curves, and $\bar{N}$ was around 4−10 for both DDAB and DDAC.[23,30] This number is too small for the surface tension curve to show a break point that is observed usually for micelle formation. However, the differential conductivity is usually very sensitive to even such small aggregates described in the literature.[3,23] Considering that $\hat{m}^{I}$does not change so much with $\hat{X}_2$ from the corresponding ones of DDAB and DDAC, designated as $\hat{m}_1^{I,0}$ and $\hat{m}_2^{I,0}$ in the following, as shown in Figure 7 and also that the mixed solutions of small aggregates and monomers are grown up into vesicles at all $\hat{X}_2$ at higher concentrations, the small aggregates were inferred to be a kind of embryo of a vesicle bilayer as suggested in our previous studies.[23,30]

Since $\hat{m}^{I}$ is nearly constant up to $\hat{X}_2 = 0.95$, addition of DDAC to the DDAB solution does not appear to affect formation of small aggregates. However, this is not true from the viewpoint of an ideal mixing. The mole fraction of chloride ions on the small aggregate surface $\hat{X}_2^{A}$at $\hat{m}^{I}$ is approximately calculated by applying[31]

$$\hat{X}_2^{A} = \hat{X}_2 - 2(\hat{X}_1\hat{X}_2/\hat{m}^{I})(\partial\hat{m}^{I}/\partial\hat{X}_2)_{T,p} \quad (6)$$

to the $\hat{m}^{I}$ vs $\hat{X}_2$ curve, and thus, we have $\hat{X}_2^{A} = \hat{X}_2$ at almost all bulk compositions. Furthermore, the $\hat{m}^{I}$ values are smaller than those estimated for ideal mixing of bromide and chloride ions on the aggregate surface at a given $\hat{X}_2$, $\hat{m}^{I,id}$, where $\hat{m}^{I,id}$ is calculated by[30]

$$\hat{m}^{I,id} = 1/\sqrt{[\hat{X}_1/(\hat{m}_1^{I,0})^2 + \hat{X}_2/(\hat{m}_2^{I,0})^2]} \quad (7)$$

Therefore, it is said that the aggregate surface is more enriched in chloride ions than expected from ideal mixing and has an almost the same composition as the monomer solution at $\hat{m}^{I}$. This forms a striking contrast to normal spherical micelles where bromide and chloride ions are mixed ideally[31,32] and therefore suggests a different morphology of small aggregates from normal spherical micelles.

Vesicle Formation of DDAB and DDAC Systems. A vesicle particle has one or several closed bilayer(s) that is constructed from an outer monolayer with a positive curvature as well as an inner monolayer with a negative one. Therefore, it is crucial for the properties and structures of vesicles to know which one of them is more affected by the difference in the degree of counterion binding between bromide and chloride ions. It is known that the degree of binding of chloride ions is less than that of bromide ions (Hofmeister series),[38] and thus, the electrostatic repulsion between head groups at the micelle surface is stronger for DTAC than for DTAB. The experiments showed the critical micelle concentration of DTAC, $(cmc)^0_{DTAC}$, is larger than that of DTAB, $(cmc)^0_{DTAB}$, and ln $(cmc)^0_{DTAC}/(cmc)^0_{DTAB} \approx 0.34$.[32] For the small aggregate formation of DDAB and DDAC, we have ln $\hat{m}_2^{I,0}/\hat{m}_1^{I,0} \approx 0.34$ from Table 1.

However, we note that the onsets of vesicle formation of the respective pure surfactants, $\hat{m}_1^{II,0}$ and $\hat{m}_2^{II,0}$, are much different from each other, and its ratio gives ln $\hat{m}_2^{II,0}/\hat{m}_1^{II,0} \approx 3.3$. This leads to $[\hat{m}_2^{II,0}/\hat{m}_1^{II,0}]/[(cmc)^0_{DTAC}/(cmc)^0_{DTAB}] \approx 20$, i.e., vesicle formation is affected by 20 times as much as micelle formation due to the difference in the degree of counterion binding. The most essential difference between vesicle and micelle particles is that the former has an inner closed monolayer with a negative curvature but the latter does not have it. Therefore, it is said that the difference in the ability of binding to surfactant headgroup cation between bromide and chloride ions has a larger influence on the inner closed monolayer than on the outer

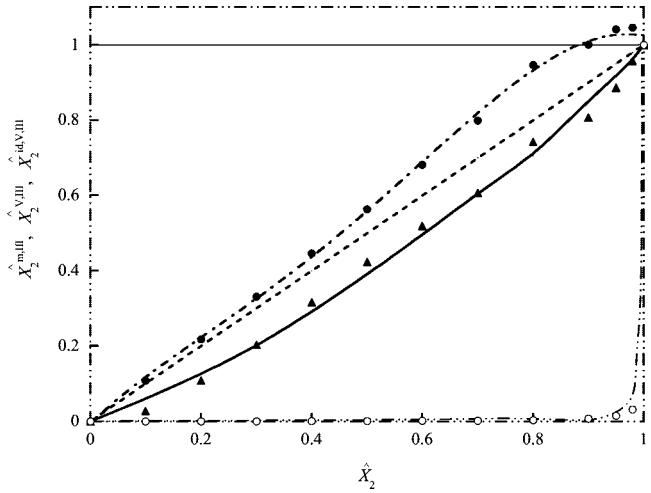

Figure 9. Compositions of monomer $\hat{X}_2^{m,III}$, vesicle $\hat{X}_2^{V,III}$, and ideal mixing in vesicle $\hat{X}_2^{id,V,III}$ vs composition $\hat{X}_2$ at $\hat{m}^{III}$: (●) $\hat{X}_2^{V,III}$, (▲) $\hat{X}_2^{m,III}$, (○) $\hat{X}_2^{id,V,III}$.

monolayer, since the inner monolayer is forced to expand by changing bromide to chloride ions and thus the size of DDAC vesicles is expected to be larger than that of DDAB, which is supported by CryoTEM images in Figure 7. From a different point of view, we note that $\ln \hat{m}_1^{II,0}/\hat{m}_1^{I,0} \approx 2.3$, but $\ln \hat{m}_2^{II,0}/\hat{m}_2^{I,0} \approx 5.2$. Therefore, small aggregates of DDAC are more stable against the increase of chemical potential than those of DDAB. This is consistent with the observation that $\hat{X}_2^A = \hat{X}_2$, and thus, the aggregate surface is more enriched in chloride ions than expected from the ideal mixing of bromide and chloride ions.

One of the conspicuous features being relevant to vesicle formation in Figure 6 is that a further increase in the chemical potential of surfactant is required for surfactants in small aggregates and monomeric state are combined to form vesicles, and eventually all the small aggregates disappear. The increase is estimated roughly to be $\Delta\mu_1^0 = RT \ln \hat{m}_1^{III,0}/\hat{m}_1^{II,0} \approx 5$ kJ mol^{-1} for DDAB and $\Delta\mu_2^0 = RT \ln \hat{m}_2^{III,0}/\hat{m}_2^{II,0} \approx 0.6$ kJ mol^{-1} for DDAC. This suggests that the growing process of small aggregates is easier, and thus, the small aggregate (a kind of embryo of bilayer structure as mentioned above) may be more similar to part of the bilayer for DDAB than for DDAC.

Vesicle Formation of the DDAB−DDAC Mixtures. The composition of vesicles at $\hat{m}^{II}$ is usually calculated using

$$\hat{X}_2^V = \hat{X}_2 - 2(\hat{X}_1\hat{X}_2/\hat{m}^{II})(\partial\hat{m}^{II}/\partial\hat{X}_2)_{T,p} \tag{8}$$

if vesicles are formed from dilute monomer solution as in the case of anionic + cationic[16] and single-chain + double-chain[23] surfactant mixtures. In the present case, however, vesicles are formed in the small aggregates + monomer solutions, and thus, eq 8 is not applicable. Similarly, the vesicle composition at $\hat{m}^{III}$ is changed from that at $\hat{m}^{II}$ and not evaluated using the analogue of eq 8. However, when we introduce some assumptions, the monomer and then vesicle compositions can be estimated as follows.

As mentioned above, the increases of chemical potentials, $\Delta\mu_1^0$ and $\Delta\mu_2^0$, are required for all the small aggregates to disappear for pure DDAB and DDAC systems and similarly $\Delta\mu = \Delta\mu_1 + \Delta\mu_2$ for the mixture, where $\Delta\mu_i$ is the contribution from the surfactant i. Here let us assume the additivity relation

$$\Delta\mu = \hat{X}_1^{m,III}\Delta\mu_1^0 + \hat{X}_2^{m,III}\Delta\mu_2^0 \tag{9}$$

where $\hat{X}_i^{m,III}$ is the mole fraction of surfactant i of monomeric state at $\hat{m}^{III}$ and designate $\hat{m}^{III}$ thus determined as $\hat{m}^{III,ad}$. Taking account of the fact that DDAB and DDAC have a common ion, $\hat{m}^{III,ad}$ is estimated (see Appendix) by

$$(\hat{m}^{III,ad}/\hat{m}^{II}) = [\hat{X}_1(\hat{m}_1^{III,0}/\hat{m}_1^{II,0})^{\hat{X}_1^{m,III}} + (\hat{X}_1 + \hat{X}_2)(\hat{m}_1^{III,0}/\hat{m}_1^{II,0})^{\hat{X}_1^{m,III}}(\hat{m}_2^{III,0}/\hat{m}_2^{II,0})^{\hat{X}_2^{m,III}} + \hat{X}_2(\hat{m}_2^{III,0}/\hat{m}_2^{II,0})^{\hat{X}_2^{m,III}}]/2 \tag{10}$$

Substituting $\hat{m}_i^{II,0}$, $\hat{m}_i^{III,0}$, and $\hat{m}^{II}$ at $\hat{X}_2$, we found $\hat{X}_i^{m,III}$ that gives a minimum of $(\hat{m}^{III,ad} - \hat{m}^{III})^2$. Here it should be noted that the difference between $\hat{X}_i$ and $\hat{X}_i^{m,III}$ is caused by an increase from $\hat{m}^{II}$ to $\hat{m}^{III}$ in which surfactants in small aggregates + monomeric states of the overall composition of $\hat{X}i$ are converted into vesicle particles of composition $\hat{X}_i^{V,III}$ + monomeric state of composition $\hat{X}_i^{m,III}$.

Once $\hat{X}_i^{m,III}$ is estimated, $\hat{X}_i^{V,III}$ is evaluated by relying on the mass balance equations

$$\hat{m}^{III} = \hat{m}^{m,III} + \hat{m}^{V,III} \tag{11}$$

and

$$\hat{m}^{III}\hat{X}_2 = \hat{m}^{m,III}\hat{X}_2^{m,III} + \hat{m}^{V,III}\hat{X}_2^{V,III} \tag{12}$$

where $\hat{m}^{m,III}$ and $\hat{m}^{V,III}$ are the total molalities of surfactants in monomeric state and vesicle particles, respectively. Since it is reasonably assumed that the total concentration of monomers does not change very much once vesicle particles are formed (phase separation approximation), $\hat{m}^{m,III} \approx \hat{m}^{II}$, $\hat{X}_2^{V,III}$ is evaluated by

$$\hat{X}_2^{V,III} = (\hat{m}^{III}\hat{X}_2 - \hat{m}^{II}\hat{X}_2^{m,III})/(\hat{m}^{III} - \hat{m}^{II}) \tag{13}$$

When bromide and chloride ions are mixed ideally, furthermore, $\hat{m}^{m,III}$ is expressed in two ways as

$$(\hat{m}^{m,III})^2 = (\hat{m}_1^{m,III,0})^2 + [(\hat{m}_2^{m,III,0})^2 - (\hat{m}_1^{m,III,0})^2]\hat{X}_2^{id,V,III} \tag{14}$$

and

$$1/(\hat{m}^{m,III})^2 = 1/(\hat{m}_1^{m,III,0})^2 + [1/(\hat{m}_2^{m,III,0})^2 - 1/(\hat{m}_1^{m,III,0})^2]\hat{X}_2^{m,III} \tag{15}$$

where $\hat{X}_2^{id,V,III}$ is $\hat{X}_2^{V,III}$ of the ideal mixing. Equations 13 and 15 and $\hat{m}_i^{m,III,0} \approx \hat{m}_i^{II,0}$ give the relation

$$X_2^{id,V,III} = (\hat{m}_1^{II,0})^2\hat{X}_2^{m,III}/[(\hat{m}_2^{II,0})^2 + \{(\hat{m}_1^{II,0})^2 - (\hat{m}_2^{II,0})^2\}\hat{X}_2^{m,III}] \tag{16}$$

The values of $\hat{X}_2^{m,III}$, $\hat{X}_2^{V,III}$, and $\hat{X}_2^{id,V,III}$ calculated from eqs 10, 13, and 16 are plotted against $\hat{X}_2$ in Figure 9. The results show $\hat{X}_2^{m,III} < \hat{X}_2 < \hat{X}_2^{V,III}$ at a given $\hat{X}_2$, i.e., vesicle surface is enriched in chloride ions compared to the monomeric state. However the difference between $\hat{X}_2^{V,III}$ and $\hat{X}_2$ is rather small similarly to the case of small aggregates as described with respect to eq 6. More surprisingly is that $\hat{X}_2^{V,III}$ is much larger than $\hat{X}_2^{id,V,III}$, where $\hat{X}_2^{id,V,III}$ is almost zero until $\hat{X}_2$ is very close to unity. In the thermodynamic phrases,[31] the excess Gibbs free energy of vesicle formation $\hat{g}^{V,E}$ is more negative ($\sim$−3 kJ mol^{-1} at its minimum) compared to those of micelle formation $\hat{g}^{M,E}$of the systems where attractive molecular interaction between different species is stronger than that between the same species in micelle.[39,40] Therefore, addition of chloride ions to DDAB vesicles as well as that of bromide ions to DDAC vesicles is favorable for vesicle formation compared to that of the respec-

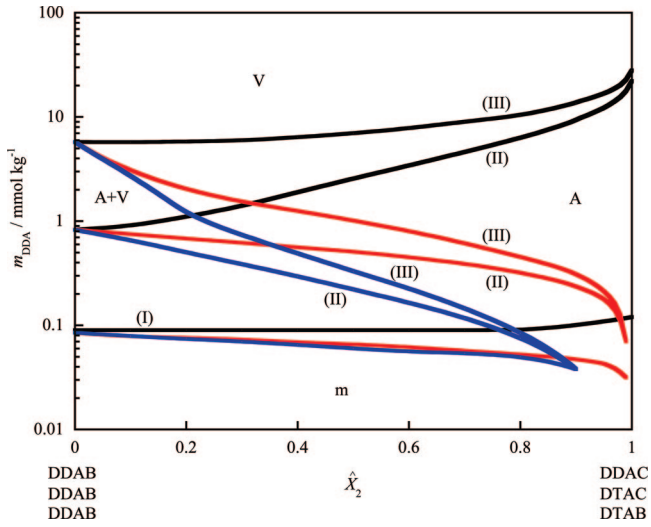

Figure 10. Concentration of double-chain surfactant ion vs composition diagrams of aggregate formation: (black lines) DDAB−DDAC, (red lines) DDAB−DTAC, (blue lines) DDAB−DTAB; (I) m_{DDA} at m^{I}, (II) m_{DDA} at m^{II}, (III) m_{DDA} at m^{III}.

tive pure surfactants. This forms a striking contrast to the almost ideal mixing of bromide and chloride ions at micelle surfaces.[31]

It has been shown that even the mixing of a surfactant that does not form vesicles alone to a surfactant that forms vesicles strongly enhances vesicle formation.[23] Bergström et al. suggested theoretically that the more the asymmetry of surfactant structures is increased, the more vesicle formation is enhanced.[26–28] These are attributable to the fact that vesicle particles have not only an outer monolayer with a positive curvature but also inner monolayer with a negative curvature and brings an uneven distribution of constituents between them. Let us closely look at this point by comparing several mixed systems.

Effect of Asymmetry of Surfactant and Counter Ions on Vesicle Formation. Since a framework of monolayers is surfactant ions, asymmetry in surfactant ion structure is expected to be more influential on vesicle formation than that in counterion. As far as we aware of, however, there is no systematic report on this point.

Figure 10 demonstrates how the concentration of DDA^+ ion at the transition points (m_D^I, m_D^{II}, and m_D^{III}) changes by mixing another surfactant with DDAB, i.e., DDA^+ is common but counterion is different (DDAB + DDAC), $Br^-$is common but surfactant ion is different (DDAB + DTAB),[23] and both ions are different from each other (DDAB + DTAC).[30]

Let us examine m_D^{II} and m_D^{III} values. Comparing the DDAB + DDAC system with the DDAB + DTAB system, we note that the m_D^{II} and m_D^{III} values for the latter are much more depressed compared to the former in spite of the DTAB not forming vesicles alone. Since DTA^+ has a cone-shaped molecular geometry and m_D^{II} and m_D^{III} are decreased, DTA^+ ions are expected to effectively and mainly fill outer monolayers. Therefore, this uneven distribution of surfactant cations between inner and outer monolayers seems to be much more influential on vesicle formation than that counterions. Taking account of the fact that the m_D^{II} and m_D^{III} values of the DDAB + DDAC system are considerably decreased from those expected from the ideal mixing, a synergistic effect due to the fact that both surfactant and counterion are different and consequently a further decrease of m_D^{II} and m_D^{III} from the DDAB + DTAB system are anticipated for the DDAB + DTAC system. However, we realize from Figure 10 that this is not the case; conversely, the m_D^{II} and m_D^{III} values for the DDAB + DTAB system are increased by introducing the asymmetry in counterions. Therefore, it is said that the uneven and suitable distribution of surfactant ions having different molecular shape between the inner and outer monolayes is primarily decisive and the asymmetry in counterion distribution is subsidiary for vesicle formation.

Appendix

Let us estimate the compositions of monomer and vesicle based on the following idea. An increment of the Gibbs free energy $\Delta\mu$ from the onset of vesicle formation (point II) to the end point of existence of small aggregates (point III) of the mixture is evaluated experimentally from $\hat{m}^{II}$ and $\hat{m}^{III}$ values as shown in Figure 6. On the other hand, $\Delta\mu$ could be estimated using a simple additivity relation in terms of the corresponding increment of the respective single surfactant systems $\Delta\mu_i^0$ and the solution composition outside of vesicles $\hat{X}_i^{m,III}$as

$$\Delta\mu^{ad} = \hat{X}_1^{m,III}\Delta\mu_1^0 + \hat{X}_2^{m,III}\Delta\mu_2^0 \quad \text{(A1)}$$

Although $\hat{X}_i^{m,III}$ is usually changed as the total surfactant concentration, an iterative calculation for the difference between $\Delta\mu$ and $\Delta\mu^{ad}$ to be minimized reasonably yields $\hat{X}_i^{m,III}$.

The chemical potential of ion i is given by

$$\mu_i = \mu_i^{\ominus} + RT\ln\gamma_i m_i \quad \text{(A2)}$$

and thus, the increments required from II to III for bromide, chloride, and surfactant ions are written, respectively, by

$$\Delta\mu_{Br} = RT\ln(\gamma_{Br}^{III}m_{Br}^{III}/\gamma_{Br}^{II}m_{Br}^{II}) = RT\ln(f_{Br}\hat{X}_1^{III}\hat{m}^{III}/\hat{X}_1^{II}\hat{m}^{II}) \quad \text{(A3)}$$

$$\Delta\mu_{Cl} = RT\ln(\gamma_{Cl}^{III}m_{Cl}^{III}/\gamma_{Cl}^{II}m_{Cl}^{II}) = RT\ln(f_{Cl}\hat{X}_2^{III}\hat{m}^{III}/\hat{X}_2^{II}\hat{m}^{II}) \quad \text{(A4)}$$

and

$$\Delta\mu_D = RT\ln(\gamma_D^{III}m_D^{III}/\gamma_D^{II}m_D^{II}) = RT\ln(f_D\hat{m}^{III}/\hat{m}^{II}) \quad \text{(A5)}$$

where $f_i \equiv \gamma_i^{III}/\gamma_i^{II}$.When the additivity relation holds, eqs A3 to A5 are rewritten by substituting $\hat{X}_i^{m,III}$ and $\hat{m}^{III,ad}$ into $\hat{X}_i^{III}$ and $\hat{m}^{III}$ and thus, we have

$$\Delta\mu^{ad} = \Delta\mu_D^{ad} + \Delta\mu_{Br}^{ad} + \Delta\mu_{Cl}^{ad}$$

$$= RT\ln(f_D\hat{m}^{III,ad}/\hat{m}^{II})(f_{Br}\hat{X}_1^{m,III}\hat{m}^{III,ad}/\hat{X}_1^{II}\hat{m}^{II})\times (f_{Cl}\hat{X}_2^{m,III}\hat{m}^{III,ad}/\hat{X}_2^{II}\hat{m}^{II}) \quad \text{(A6)}$$

Similary, for the respective single-surfactant systems, the increment of ion i is given by

$$\Delta\mu_i^0 = RT\ln(f_i^0\hat{m}_i^{III,0}/\hat{m}_i^{II,0}) \quad \text{(A7)}$$

and thus, we have

$$\Delta\mu^{ad} = \hat{X}_1^{m,III}(\Delta\mu_{Br}^0 + \Delta\mu_{D,1}^0) + \hat{X}_2^{m,III}(\Delta\mu_{Cl}^0 + \Delta\mu_{D,2}^0)$$

$$= RT\ln(f_{Br}^0 f_{D,1}^0\hat{m}_1^{III,0}/\hat{m}_1^{II,0})^{2\hat{X}_1^{m,III}}(f_{Cl}^0 f_{D,2}^0\hat{m}_2^{III,0}/\hat{m}_2^{II,0})^{2\hat{X}_2^{m,III}} \quad \text{(A8)}$$

Equations A6 and A8 yield the total concentration $\hat{m}^{III,ad}$ that describes the addtitivity relation as

$$(\hat{m}^{\mathrm{III,ad}}/\hat{m}^{\mathrm{II}}) = [\hat{X}_1(\hat{m}_1^{\mathrm{III},0}/\hat{m}_1^{\mathrm{II},0})^{\hat{X}_1^{\mathrm{m,III}}} + (\hat{X}_1 + \hat{X}_2)(\hat{m}_1^{\mathrm{III},0}/\hat{m}_1^{\mathrm{II},0})^{\hat{X}_1^{\mathrm{m,III}}}(\hat{m}_2^{\mathrm{III},0}/\hat{m}_2^{\mathrm{II},0})^{\hat{X}_2^{\mathrm{m,III}}} + \hat{X}_2(\hat{m}_2^{\mathrm{III},0}/\hat{m}_2^{\mathrm{II},0})^{\hat{X}_2^{\mathrm{m,III}}}]/2 \quad \text{(A9)}$$

where we assumed that the activity coefficient of ions in the mixture is nearly equal to those in the respective single-surfactant systems at the same concentration. Thus, substituting $\hat{m}_i^{\mathrm{II},0}$, $\hat{m}_i^{\mathrm{III},0}$ and $\hat{m}^{\mathrm{II}}$ at a given $\hat{X}_i$ and then minimizing $\hat{m}^{\mathrm{III,ad}} - \hat{m}^{\mathrm{III}}$ yields $\hat{X}_i^{\mathrm{m,III}}$ at the $\hat{X}_i$.

The idea given above is applicable also other combinations of binary surfactants. The final equations corresponding to eq A9 are derived as follows: for nonionic(R_1)−nonionic(R_2) mixtures

$$(m^{\mathrm{III,ad}}/m^{\mathrm{II}}) = [X_1(m_1^{\mathrm{III},0}/m_1^{\mathrm{II},0})^{X_1^{\mathrm{m,III}}} + X_2(m_2^{\mathrm{III},0}/m_2^{\mathrm{II},0})^{X_2^{\mathrm{m,III}}}] \quad \text{(A10)}$$

where $m = m_1 + m_2$ and $X_2 = m_2/m$. For nonionic(R_1)−ionic ($R_2^+X^-$) mixtures and ionic ($R_1^+Y^-$)−ionic ($R_2^+X^-$) mixtures without a common ion, apparently the same formula

$$(\hat{m}^{\mathrm{III,ad}}/\hat{m}^{\mathrm{II}}) = [\hat{X}_1(m_1^{\mathrm{III},0}/m_1^{\mathrm{II},0})^{\hat{X}_1^{\mathrm{m,III}}} + \hat{X}_2(m_2^{\mathrm{III},0}/m_2^{\mathrm{II},0})^{\hat{X}_2^{\mathrm{m,III}}}] \quad \text{(A11)}$$

holds where $\hat{m} = m_1 + 2m_2$ and $\hat{X}_2 = 2m_2/m$ for the former, whereas $\hat{m} = 2m_1 + 2m_2$ and $\hat{X}_2 = 2m_2/m$ for the latter.

Acknowledgment. This work was supported in part by a Grant-in-Aid for Scientific Research (B) (no. 1635005) and also by a Grant-in-Aid for Scientific Research on Priority Area (No.18445026) from the Ministry of Education, Science, Sports and Culture. The authors wish to express their gratitude to Prof. Masahiko Abe and Prof. Hideki Sakai of Tokyo University of Science for permission to perform the cryoTEM experiments at the facility of their research group.

References and Notes

(1) Matsumoto, T. *Colloid Polym. Sci.* **1992**, *270*, 492.
(2) Caria, A.; Regev, O.; Khan, A. *J. Colloid Interface Sci.* **1998**, *200*, 19.
(3) Kawamura, H.; Manabe, M.; Nomura, M.; Inoue, T.; Murata, Y.; Sasaki, Y. *Nippon Kagaku Kaishi* **1996**, *10*, 861.
(4) Svitova, T. F.; Smirnova, Y. P.; Pisarev, S. A.; Berezina, N. A. *Colloids Surf. A* **1995**, *98*, 107.
(5) Cantù, L.; Corti, M.; Favero, E. D.; Raudino, A. *J. Phys. II Fr.* **1994**, *4*, 1585.
(6) Talmon, Y.; Evans, D. F.; Ninham, B. W. *Science* **1983**, *221*, 1047.
(7) Israelachivili, J. *Intermolecular & Surface Forces*, 2nd ed.; Academic Press: San Diego, CA, 1991; p 378.
(8) Helfrich, W. *Z. Naturforsch.* **1973**, *28c*, 693.
(9) Safran, S. A. *Statistical Thermodynamics of Surfaces, Interfaces, and Membranes*; Perseus Books: Massachusetts, 1994.
(10) Bergström, L. M. *Langmuir* **2006**, *22*, 3678.
(11) Villeneuve, M.; Kaneshina, S.; Aratono, M. *J. Colloid Interface Sci.* **2001**, *239*, 254.
(12) Lusvardi, K. M.; Full, A. P.; Kaler, E. W. *Langmuir* **1995**, *11*, 487.
(13) Viseu, M. I.; Edwards, C. S.; Campos, C. S.; Costa, S. M. B. *Langmuir* **2000**, *16*, 2105.
(14) Viseu, M. I.; Velazquez, N. M.; Campos, C. S.; Garcia-Mateos, I.; Costa, S. M. B. *Langmuir* **2000**, *16*, 4882.
(15) Treiner, C.; Makayssi, A. *Langmuir* **1992**, *8*, 794.
(16) Villeneuve, M.; Kaneshina, S.; Imae, T.; Aratono, M. *Langmuir* **1999**, *15*, 2029.
(17) Kaler, E. W.; Herrington, K. L.; Murthy, A. K.; Zasadzinski, J. A. N. *Science* **1989**, *245*, 1371.
(18) Kaler, E. W.; Herrington, K. L.; Miller, D. D.; Zasadzinski, J. A. N. *Structure and Dynamics of Strongly Interacting Colloids and Supramolecular Aggregates in Solution*; Chen, S.-H., et al., Eds.; Kluwer Academic Publishers: Amsterdam, 1992; p 571.
(19) Dragèeviæ, Ð.; Bujan, M.; Grahek, Z.; Filipoviæ-Vincekoviæ, N. *Colloid Polym. Sci.* **1995**, *273*, 967.
(20) Tomašiæ, V.; Štefaniæ, I.; Filipoviæ-Vincekoviæ, N. *Colloid Polym. Sci.* **1999**, *277*, 153.
(21) Iampietro, D. J.; Kaler, E. W. *Langmuir* **1999**, *15*, 8590.
(22) Tondre, C.; Caillet, C. *Adv. Colloid Interface Sci.* **2001**, *93*, 115.
(23) Aratono, M.; Onimaru, N.; Yoshikai, Y.; Shigehisa, M.; Koga, I.; Wongwailikhit, K.; Ohta, A.; Takiue, T.; Lhoussaine, B.; Strey, R.; Takata, Y.; Villeneuve, M.; Matsubara, H. *J. Phys. Chem. B* **2007**, *111*, 107.
(24) Feiosa, E.; Alves, F. R.; Niemiec, A.; Oliveira, M. E. C. D.; Csstanheira, E. M. S.; Baptista, A. L. F. *Langmuir* **2006**, *22*, 3579.
(25) Safran, S. A.; Pincus, P.; Andelman, D. *Science* **1990**, *248*, 354.
(26) Safran, S. A. *Adv. Phys.* **1999**, *48*, 395.
(27) Bergström, L. M.; Eriksson, J. C. *Langmuir* **1996**, *12*, 624.
(28) Bergström, L. M. *J. Colloid Interface Sci.* **2001**, *240*, 294.
(29) Bergström, L. M. *Langmuir* **2006**, *22*, 6796.
(30) Aratono, M.; Koga, I.; Shigehisa, M.; Onimaru, N.; Takiue, T.; Matsubara, H. Unpublished data.
(31) Aratono, M.; Villeneuve, M.; Takiue, T.; Ikeda, N.; Iyota, H. *J. Colloid Interface Sci.* **1998**, *200*, 161.
(32) Yamanaka, M.; Amano, M.; Ikeda, N.; Aratono, M.; Motomura, K. *Colloid Polym. Sci.* **1992**, *270*, 682.
(33) Capiciani, A.; Germani, R.; Savelli, G.; Bunton, C. A.; Mhala, M.; Moffatt, J. R. *J. Chem. Soc., Parkin Trans. II* **1987**, 541.
(34) Sadar, M. J. *Technical Information Series - Booklet No.11*; Hach Co.: USA, 1998.
(35) Hunter, R. J. *Introduction to Modern Colloid Science*; Oxford University Press: England, U.K., 1993.
(36) Evans, D. F.; Ninham, B. W. *J. Phys. Chem.* **1986**, *90*, 226.
(37) Murakami, R.; Takata, Y.; Ohta, A.; Takiue, T.; Aratono, M. *J. Colloid Interface Sci.* **2004**, *270*, 262.
(38) Evans, D. F.; Wennerström, H. *The Colloidal Domain*, 2nd ed.;Wiley-VCH: New York, 1999; p 130.
(39) Matsubara, H.; Ohta, A.; Kameda, M.; Villeneuve, M.; Ikeda, N.; Aratono, M. *Langmuir* **1999**, *15*, 5496.
(40) Matsubara, H.; Ohta, A.; Kameda, M.; Ikeda, N.; Aratono, M. *Langmuir* **2000**, *16*, 7589.

JP803484B